

V-f and P-Q Control of Solar Photo Voltaic Generators with MPPT and Battery Storage

K. Chandrasekhar

Department of Electrical and Electronics Engineering,
Andhra University College of Engineering (A),
Andhra University, Visakhapatnam,
Andhra Pradesh 530003, India.

N. Raghunadh

Department of Electrical and Electronics Engineering,
Andhra University College of Engineering (A),
Andhra University, Visakhapatnam,
Andhra Pradesh 530003, India.

Abstract

The microgrid concept allows small distributed energy resources to act in a coordinated manner to provide a necessary amount of active and reactive power when required. This paper discusses control of solar PV generators with the maximum power point tracking (MPPT) control and battery storage control to provide voltage and frequency (V-f) support to an islanded microgrid. Also, active and reactive power (P-Q) control with solar PV, MPPT and battery storage is proposed for the grid connected mode. The control strategies show effective coordination between inverter V-f (or P-Q) control, MPPT control, and energy storage charging and discharging control. The simulation studies are carried out with the distribution bus feeder test system in grid connected and islanded microgrid modes. The results clearly verify the effectiveness of proposed control methods. The simulations are carried out in Matlab and Sim power systems.

Index Terms—distributed generation (DG), solar photovoltaic (PV) maximum power point tracking (MPPT), Perturb and Observe (P&O) algorithm, Battery storage control, voltage and frequency (V-f) control, active and reactive power (P-Q) control.

I. INTRODUCTION

The microgrid is a collection of distributed generators or micro resources, energy storage devices, and loads which operate as a single and independent controllable system capable of providing power to the area of service. The micro resources that are incorporated in a micro grid

are comprised of small units, less than 100 kW, provided with power electronics interface. Most common resources are Solar Photo voltaic (PV), Fuel Cell, or micro turbines connected at the distribution voltage level.

In a micro grid, the micro sources and storage devices are connected to the feeders through the micro source controllers and the coordination among the micro sources is carried out by the central controller. The micro grid is connected to the medium voltage level utility grid at the point of common coupling (PCC) through the circuit breakers. When a microgrid is connected to the grid, the operational control of voltage and frequency is done entirely by the grid. However, a microgrid still supplies the critical loads at PCC, thus, acting as a PQ bus. In islanded condition, a microgrid has to operate on its own, independent of the grid, to control the voltage and frequency of the microgrid and hence, acts like a PV (power-voltage) bus. The operation and management in both the modes is controlled and coordinated with the help of micro source controllers at the local level and central controller at the global level.

The operation and control of the inverter interface of renewable based distributed energy resources, like Solar Photovoltaic in a microgrid, is a real challenge, especially when it comes to maintaining both microgrid voltage and frequency within an acceptable range. A

Cite this article as: K. Chandrasekhar & N. Raghunadh, "V-f and P-Q Control of Solar Photo Voltaic Generators with MPPT and Battery Storage", International Journal & Magazine of Engineering, Technology, Management and Research, Volume 6 Issue 8, 2019, Page 89-101.

voltage control method based on traditional droop control for voltage sag mitigation along with voltage ride through capability is proposed in [3]. A dynamic voltage regulation based on adaptive control is proposed in [4], [5]. However, there are not many research works performed on V-f or P-Q control using solar PV including MPPT control and battery storage in microgrids. In [6], frequency regulation with PV in microgrids is studied; however, this work does not consider the voltage control objective and lacks battery storage in the microgrid.

In [7], a small scale PV is considered in a grid-connected mode to control the active and reactive power of the system. Here, the control methods consider abc-dq0 transformation and vice versa which is avoided in the present paper. In [8], power modulation of solar PV generators with an electric double layer capacitor as energy storage is considered for frequency control. In [9], load frequency control is implemented in microgrid with PV and storage. However, this work also lacks the consideration of a voltage control objective. In summary, the previous works in this topic either lack the incorporation of an energy storage component or the voltage control objective along with frequency control or the incorporation of control transition in different scenarios. The present work fulfills these gaps by considering all of these objectives.

This paper discusses several control algorithms through which the capability of PV generators for voltage and frequency (V-f) control and active and reactive power (P-Q) control in islanded and grid connected microgrids could be harnessed. Detailed models of PV, battery, inverter and converter are considered for the study. MPPT control at the PV side, battery control, and V-f/P-Q control algorithm at the inverter side, these three control algorithms at three stages are jointly linked through a power balance objective at the DC and AC side of the inverter so that the DC side voltage is indirectly controlled at the desired value in order to maintain the AC side voltage at the utility desired voltage. At the same time, the controls can seamlessly transform from

one mode e.g., inverter P-Q control in grid connected mode to V-f control in islanded mode. The proposed control methods are validated with satisfactory results. The controls are developed in abc reference frames using the RMS values of voltages and active and reactive power. Hence, it is easy and efficient to implement, and avoids the transformation to and from other reference frames which greatly simplifies the control strategies. The chosen control parameters in the proposed methodologies are, however, dependent on the PV, battery, and external power grid conditions. These parameters can be adaptively achieved with the changing system conditions which could be a very promising future direction of this work.

The rest of the paper is organized as follows: Section III briefly presents the analytical modeling of Solar PV with model validation results. Section IV shows the PV system configuration, describes the modeling of the battery storage, and provides information about the structure of distribution feeder under study. Section V describes the proposed coordinated V-f and P-Q control algorithms while incorporating PV MPPT control and battery storage control. Section VI presents convincing results to prove the effectiveness of the proposed control algorithms. Finally, Section VII summarizes the major contributions of the paper.

II. SOLAR PV MODELING AND VALIDATION

An array of photovoltaic (PV) modules is implanted by PV Array block of Simscape Power System family. The array is built of strings of modules connected in parallel, each string consisting of modules connected in series. This block allows to model pre-set PV modules from the National Renewable Energy Laboratory (NREL) System Advisor Model (Jan. 2014) as well as PV modules that user define.

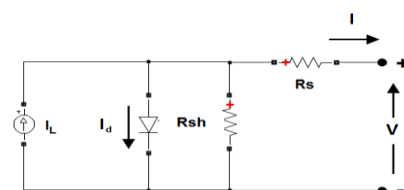


Fig (1). Equivalent model of solar PV

The equivalent model of solar PV Array shown in Fig(1) is a five parameter model using a current source I_L (light-generated current), I_0 (diode current), n_1 (diode ideality factor), R_S (series resistance), and R_{Sh} (shunt resistance) to represent the irradiance and temperature dependent I-V characteristics of the modules. The diode I-V characteristics for a single module are defined by the equations (1) and (2)

$$I_d = I_o \left(e^{\left(\frac{v_d}{V_T} \right)} - 1 \right) \quad (1)$$

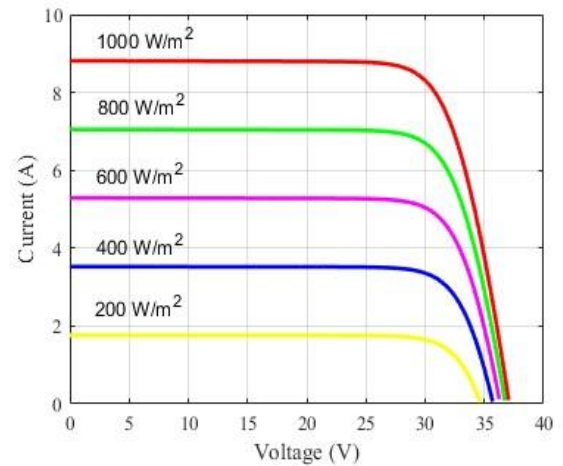
$$V_T = \frac{KT}{q} \times n_1 \times N_{cell} \quad (2)$$

Where I_d is diode current (A), I_0 diode saturation current (A), V_d diode voltage (V), V_T terminal voltage (V), K is Boltzmann's constant ($1.3806 \times 10^{-23} \text{ J.K}^{-1}$), T is cell temperature (Kelvin), q is charge of electron ($1.6022 \times 10^{-19} \text{ C}$) n_1 diode ideality factor (number usually chosen in range 1.0 to 1.5) and N_{cell} number of cells connected in series in module.

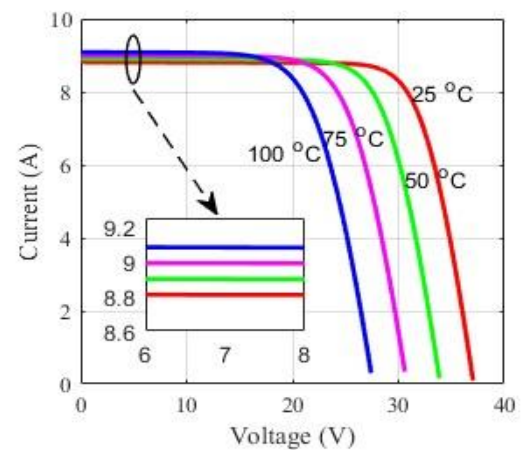
Model	LG250S1C-G2
Peak Power (P_{max})	250.26 Watts
Voltage @ Peak Power (V_{mpp})	37.1 Volts
Current @ Peak Power (I_{mpp})	8.76 Amps
Open circuit Voltage (V_{oc})	29.9 Volts
Short Circuit current (I_{sc})	8.37 Amps
Cells per module (N_{cell})	60

Table (1). PV panel parameters (1000 W/m^2 Irradiance and 25°C Temperature)

Using these fundamental equations and parameters from the data sheet, the PV model is developed and verified with the panel datasheet. The I-V characteristics of LG250S1C-G2 for different irradiance levels at the cell temperature of 25°C and varying cell temperature for a constant irradiance level of 1000 W/m^2 as obtained from the simulation are shown in Figs. 2(a) and 2(b), respectively. The similarities of the I-V curves for different conditions with the corresponding curves in the LG250S1C-G2 panel datasheet prove the validity of the developed solar panel model. The parameters of the PV panel under study are shown in Table I.



(a)



(b)

Fig (2). The I-V characteristics of LG250S1C-G2 from simulation with (a) varying irradiance at a cell temperature of 25°C and; (b) varying cell temperature at 1000 W/m^2 .

The PV system under study has 31 parallel strings with each string having 13 series connected panels. The voltage and current of PV array is increased by increasing series and parallel modules. The Maximum Power Point (MPP) for a single panel of LG250S1C-G2 at 1000 W/m^2 irradiance and 25°C temperature (STC) is 250.26W. Hence, the maximum power of the PV generator at STC is $13 \times 31 \times 250.26 = 100 \text{ kW}$ (approximately). This was justified by the fig (3) with maximum power as 100KW.

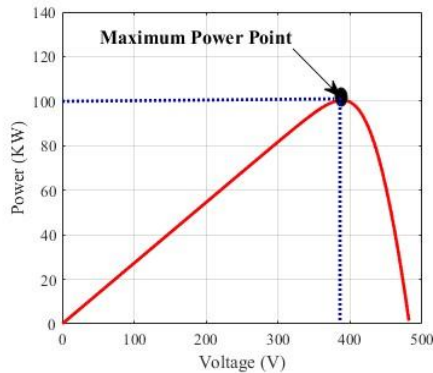


Fig (3). Maximum power at Standard Test Conditions (1000 W/m² irradiance and 25°C temperature)

III. SYSTEM CONFIGURATION AND SYSTEM DESCRIPTION

PV System Configuration:

Fig. 4 shows the PV system configuration for V-f and P-Q control with PV operating at MPP including the battery storage backup. It is a two-stage configuration where a DC-DC boost converter is used for MPPT control. The system also considers a battery back-up in case of emergencies while maintaining the voltage and frequency of the microgrid or while trying to supply the critical loads. A battery is connected in parallel to the PV to inject or absorb active power through a bidirectional DC-DC converter. When the battery is absorbing power, the converter operates in the buck mode and when battery is injecting power to the grid, it operates in the boost mode. The operation mode is maintained through the control signal provided to the converter switches.

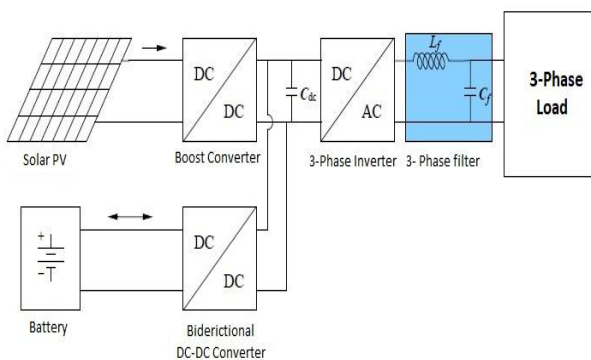


Fig (4): Battery connected standalone PV system

The PV system is connected to the grid through a filter. The filter filters out the ripples in the PV output current. The connection point is called the point of common coupling (PCC) and the PCC voltage is denoted as $v_t(t)$. The rest of the system in Fig. 4 denotes the distribution feeder which is simplified as a substation with the feeder equivalent impedance. The PV source is connected to the DC link of the inverter with a capacitor. The PV is the active power source, and the capacitor is the reactive power source of the PV system. According to the instantaneous power definitions, for a balanced three-phase system, if and denote the instantaneous PCC voltage and the inverter output voltage (harmonics neglected), respectively, then the average power of the PV denoted as $P(t)$, the apparent power $S(t)$ and the average reactive power $Q(t)$ of the PV are as given below

$$P(t) = \frac{2}{T} \int_{t-\frac{T}{2}}^t v_t(\Gamma) i_c(\Gamma) d\Gamma = \frac{V_t(t) V_c(t)}{\omega L_c} \sin \alpha \quad (3)$$

$$S(t) = V_t(t) I_c(t) = \frac{v_t(t)}{\omega L_c} \sqrt{V_t(t)^2 + V_c(t)^2 - 2V_t(t)V_c(t) \cos \alpha} \quad (4)$$

$$Q(t) = \sqrt{S^2(t) - P^2(t)} = \frac{V_t(t)}{\omega L_c} (V_c(t) \cos \alpha - V_t(t)) \quad (5)$$

Here, α is the phase angle of $v_c(t)$ relative to the PCC voltage. $P(t)$ and $Q(t)$ in (3) and (5) can be approximated by the first terms of the Taylor series if the angle α is small, as shown in (6) and (7):

$$P(t) \approx \frac{V_t(t) V_c(t)}{\omega L_c} \alpha \quad (6)$$

$$Q(t) \approx \frac{V_t(t)}{\omega L_c} (V_t(t) - V_c(t)) \quad (7)$$

Battery Modeling:

Modeling of Battery has very important role for simulation of PV system where it is used to maintain power balance between generation and demand. The battery model is taken from the MATLAB SimPowerSystems library with appropriate parameters which will be able to store or deliver 100KW power for

one hour. In this work a generic battery model of lead-acid battery is used as it is more convenient for renewable systems because of its low cost and availability in large size. By using the charging and discharging equation the lead-acid battery is modelled and this model is well accepted for use in simulation of renewable sources like PV system. From the above equivalent circuit, where

For discharging

$$V_{bat} = E - i.R_b - K \frac{Q}{Q-i.t} (i.t + i^*) + Exp(t) \quad (8)$$

For charging

$$V_{bat} = E - i.R_b - K \frac{Q}{i.t-0.1.Q} i^* - K \frac{Q}{Q-i.t} .i.t + Exp(t) \quad (9)$$

Where, V_{bat} is the actual battery voltage, E is the controlled voltage (V), i is the charging or discharging current of battery (A), R_b is the internal resistance of the battery (Ω), i^* is the filtered battery current (A), $i = \int idt$ is the actual battery charge, K is the polarization constant (V/Ah), Q is the battery capacity (Ah), A is the exponential zone amplitude (V), and B is the exponential zone time constant inverse (Ah)⁻¹. This exponential zone can be represented by a non-linear dynamic equation;

$$Exp(t) = B \cdot |i(t)| \cdot (-Exp(t)) + Au(t) \quad (10)$$

Here $Exp(t)$ =exponential zone voltage (V), $i(t)$ =battery current, $u(t)$ =charge or discharge mode ($u(t) = 0$ for discharge mode and $u(t) = 1$ for charge mode).

The size of the battery is selected to provide a maximum backup power to compensate for the PV generation in the case of a very small or no irradiance level. In this work, the MPP of PV generator at STC is 100 kW. Hence, the battery is chosen to provide this amount of power for a maximum of 1 hour with an energy content of 100 kWh. The battery backup is considered for short duration applications like frequency control and supplying power to critical loads in the event of emergency situations. One hour of battery backup is considered to be enough for other backup generators to take over the controls in the microgrid emergency situations.

IV.CONTROL METHODS

MPPT control

Eq 11. describes the Perturb and Observe(P&O) algorithm for MPPT. It generates a reference voltage which is compared with the desired PV voltage to get perturbations. The continuous perturbation affects the net voltage of boost converter resulting in change in the effective resistance of the converter. The solar PV array is optimised when the effective resistance of the array matches with that of the converter. The governing equations of the controller are as

$$V_{PV}(k) = V_{PV}(k - 1) - \Delta V$$

When

$$\left\{ \begin{array}{l} P_{PV}(K) < P_{PV}(K-1) \ \& \ V_{PV}(K) > V_{PV}(K-1) \\ P_{PV}(K) > P_{PV}(K-1) \ \& \ V_{PV}(K) < V_{PV}(K-1) \end{array} \right\}$$

$$V_{PV}(k) = V_{PV}(k - 1) + \Delta V$$

when

$$\left\{ \begin{array}{l} P_{PV}(K) < P_{PV}(K-1) \ \& \ V_{PV}(K) < V_{PV}(K-1) \\ P_{PV}(K) > P_{PV}(K-1) \ \& \ V_{PV}(K) > V_{PV}(K-1) \end{array} \right\} \quad (11)$$

where $V_{PV}(k)$ is the reference voltage generated after perturbation, i.e. present voltage, $V_{PV}(k - 1)$ is the voltage prior to perturbation, i.e. previous voltage, $P_{PV}(k)$ is the present power and $P_{PV}(k - 1)$ is the previous power. Four feasible operating points are achieved from this algorithm.

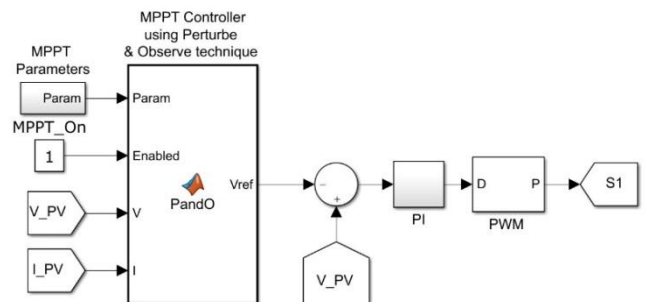


Fig (5). MPPT Control

To achieve maximum power, the duty cycle for the converter maintains the input voltage equal to the desired voltage obtained from the P&O algorithm through a PI controller. where V_{PV}^* is the reference voltage generated through MPPT controller. V_{PV} is the PV voltage of the solar array.

V-f control of inverter

Feedback PI controller PI₂ is used for voltage control at AC side. As shown in the control diagram in Fig (6), the PCC voltage is measured and the rms value of v_i(t) is calculated. Then, the rms value V_i(t) is compared to a voltage reference V_t^{*}(t) which could be a voltage specified by the utility, and the error is fed to a PI controller. The inverter output voltage v_c^{*}(t) is controlled so that it is in phase with the PCC voltage, and the magnitude of the inverter output voltage is controlled so that the PCC voltage is regulated at a given level V_t^{*}(t). The control scheme can be specifically expressed as (12).

$$v_{ci}^*(t) = v_i(t)[1 + K_{p2}(V_t^*(t) - V_i(t))] + K_{I2} \int_0^t (V_t^*(t) - V_i(t)) dt \tag{12}$$

Where K_{p2} and K_{I2} are the controller gains for this loop.

In (12), 1 has been added to the right-hand side such that when there is no injection from the PV generator, the PV output voltage is exactly the same as the terminal voltage.

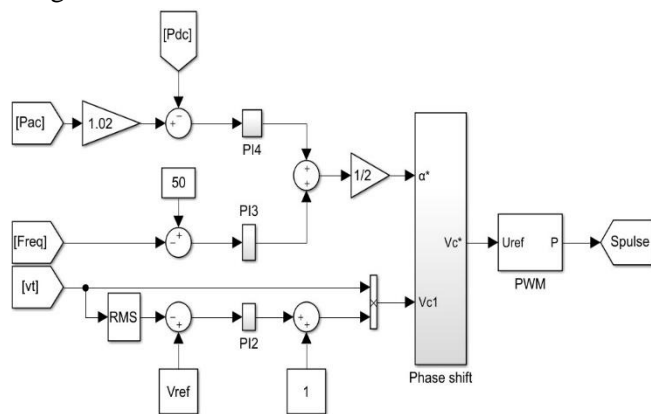


Fig (6). Inverter V-f Control

The frequency control is carried out by controlling the activepower output at the inverter side. The referenced microgrid frequency of 50 Hz is compared with the measured value and this error is fed to the PI controller that provides the phase shift contribution α₁^{*} which shifts the voltage waveform in timescale such that the active power injected will be enough to maintain the frequency at 50 Hz nominal value. The equation for this control is given by (13)

$$\alpha_1^* = K_{p3}(f_{ref} - f_{actual}) + K_{I3} \int_0^t (f_{ref} - f_{actual}) dt \tag{13}$$

There is another controller PI₄ used. This controller maintains active power balance between the AC and DC sides of the inverter. The reference signal for PI₄ is obtained from the dynamically changing active power injection from the inverter at the AC side as determined by the output of PI₃. The measured AC side active power P_{ACmeasured}, is multiplied by a factor of 1.02 considering the efficiency of inverter as 98% such that the DC side active power is 102% of the AC side active power. The DC side active power is compared with this value of AC side power and the error is fed to PI₄ to obtain the phase shift contribution from this loop as α₂^{*}. The equation for this control is given by (14)

$$\alpha_2^* = K_{p4}(1.02 \times P_{ACmeasured} - P_{DC}) + K_{I4} \int_0^t (1.02 \times P_{ACmeasured} - P_{DC}) dt \tag{14}$$

The phase shift contributions from DC and AC sides, α₁^{*} and α₂^{*} are then averaged as given by (15) to obtain the final phase shift, α^{*} of the voltage waveform, v_{c1}^{*} which, then, generates the voltage reference signal v_c^{*} for the inverter PWM

$$\alpha^* = \frac{\alpha_1^* + \alpha_2^*}{2} \tag{15}$$

Here, the reason behind considering phase shift contributions from both DC and AC side active power is to control the DC side voltage and achieve the desired value. By making α₁^{*} and α₂^{*} close in range through the controller gains, it can be assured that the active power at the DC and AC sides is balanced. This, coupled with the voltage control loop, assures that the DC side voltage is maintained at the value desired by the AC side voltage.

Battery control

The battery is incorporated in the PV system configuration in order to supply or absorb active power and support the frequency control objective with the PV generator. If there is abundant solar power and the active power required for frequency control is less than PV MPP, then the battery will be charged. If there is not enough solar power available and if the active power

required for frequency control is more than PVMPP, then the battery will supply the deficit power in order to maintain the microgrid frequency at 50 Hz. Hence, the control method for the battery charge/discharge that depends on this requirement is developed as shown in Fig. 7.

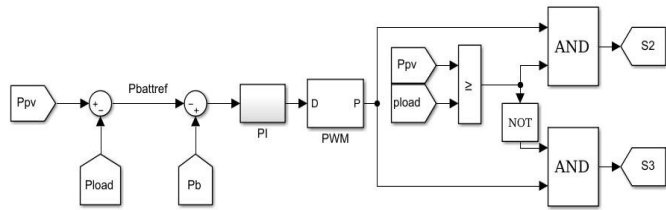


Fig (7). Battery Power Control

In Fig. 7, the reference power to the battery, $P_{Battref}$ is generated dynamically by subtracting the inverter active power injection, $P_{inverter}$ from the power generated by PV, P_{PV} . The controller comprised of a PI controller, PI_5 which receives the error signal obtained after subtracting the actual battery power, P_{batt} from the battery reference, $P_{Battref}$. The signal obtained from PI_5 is S^* , is applied to Pulse Width Modulation (PWM) in inverter controls. K_{P5} and K_{I5} are the proportional and integral gains respectively. The equation for this control is given by (16)

$$S^*(t) = K_{p5}(P_{Battref} - P_{Batt}) + K_{I5} \int_0^t (P_{Battref} - P_{Batt}) dt \tag{16}$$

One more step is considered to differentiate the charging and discharging mode of the battery. This is undertaken by comparing P_{pv} with $P_{inverter}$. If $P_{pv} \geq P_{inverter}$, the battery is in charging mode, hence, the signal obtained from the PWM, S^* and the result of this comparison is passed through a logical AND to generate a switching signal which activates the Buck mode of the DC-DC converter. If $P_{pv} < P_{inverter}$, the opposite of this signal and is passed through a logical AND to generate a switching signal which activates the Boost mode of the DC-DC converter. Hence, with this control logic, the converter is capable of operating in both directions and therefore, effectively charging and discharging the battery whenever required.

P-Q Control Method

Either in grid connected or islanded mode, the micro resources may be required to supply critical loads like hospitals, industries, etc. The proposed control strategy is applicable particularly for such cases. Fig. 8 shows the P-Q control blocks only, leaving behind the MPPT control and battery control blocks which are also present in the entire integrated control system.

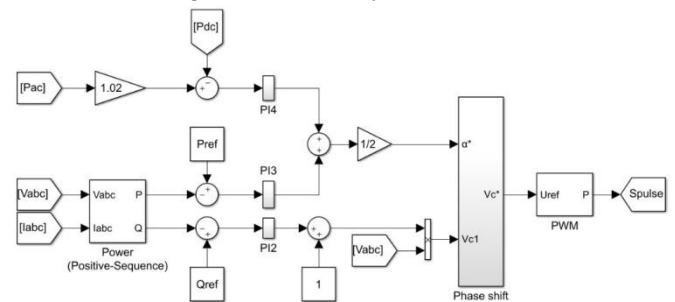


Fig (8). P-Q control diagram

The inverter side P-Q control is slightly modified version of inverter V-f control. It is entirely based on the relationship of active and reactive power at PCC with inverter output phase and voltage magnitude as given by the (6) and (7), respectively. In Fig. 8, the measured reactive power injection at PCC is compared with the referenced reactive load and this error signal is passed to the PI controller, PI_2 . Then, the term obtained is multiplied by the terminal voltage v_t to obtain the reference voltage v_{c1}^* which is in phase with v_t . The control loop 3 in Fig. 8 handles active power control through the controller PI_3 to generate the phase shift contribution α_1^* and at the same time insure the active power balance between AC and DC sides through the controller, PI_4 . This is already explained in detail in Section V-A for V-f control. Thus, the equations for P-Q control are given by (17)–(20)

$$v_{c1}^*(t) = v_t(t) [1 + K_{p2}(Q_{ref} - Q_{actual}) + K_{I2} \int_0^t (Q_{ref} - Q_{actual}) dt] \tag{17}$$

$$\alpha_1^* = K_{p3}(P_{ref} - P_{actual}) + K_{I3} \int_0^t (P_{ref} - P_{actual}) dt \tag{18}$$

$$\alpha_2^* = K_{p4}(1.02 \times P_{AC_{connected}} - P_{DC}) + K_{I4} \int_0^t (1.02 \times P_{AC_{connected}} - P_{DC}) dt \tag{19}$$

$$\alpha^* = \frac{\alpha_1^* + \alpha_2^*}{2} \quad (20)$$

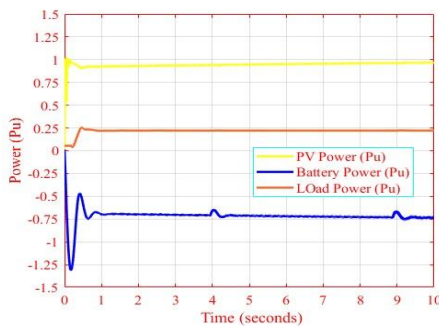
Equation (17) represents the reactive power control loop, (18) represents the active power control loop, and (19) ensures the active power balance between the DC and AC sides of the inverter. Equation (20) averages the phase shift contribution obtained from the active power control at the AC and DC sides such that the active power control at AC side and power balance objectives are taken into account.

V. SIMULATION RESULTS

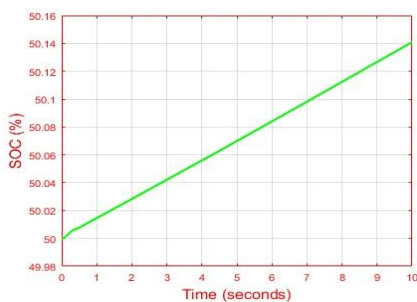
Simulation results of V-f control

For the demonstration of the V-f control algorithm, three different cases are considered: Case-I PV generated power is more than load power. As generated power is more the excess power is stored on the battery. Case-II is PV power generated is less than load power. As load power is more battery is discharge the stored energy. Case-III is PV power generated is equal to load power. As load power and PV power are equal there is no charging or discharging in this case.

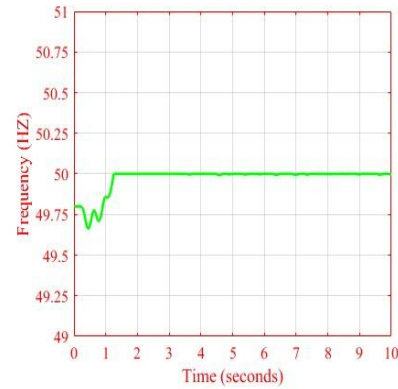
Case-I: PV power is more than load power



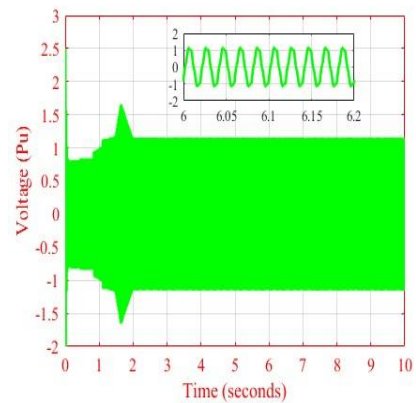
(a)



(b)



(c)



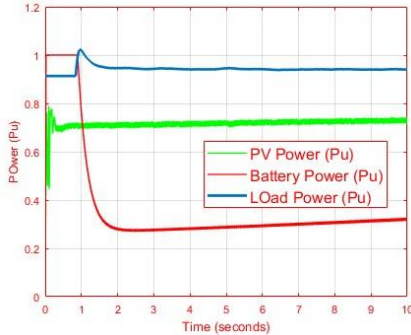
(d)

Fig 8). (a)Power (Pu) (b) SOC (%) (c) Frequency (Hz) (d) Positive sequence Voltage (Pu) while PV power is more than load power

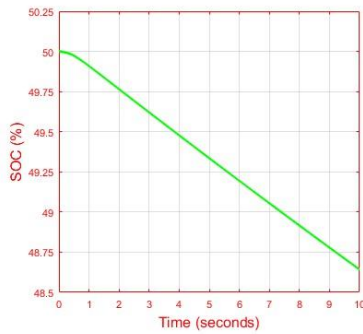
When PV power is more than load power the excess power is stored in battery storage system by charging the battery. This can be explained by using fig 8(a) and fig 8(b). In fig 8(a) Pu PV power is more than load power.

So the excess power is stored in battery by charging. The negative power indicates the charging of battery. In fig 8(b) SOC increasing with time indicates the charging of battery. Fig.8(c) and 8(d) shows the frequency which initially dips to a value of 49.75Hz due to the load-generation imbalance. The frequency control from the PV generator starts within 2sec which quickly regulates the frequency back to 50Hz. Fig 8(d) shows the plot of the PCC voltage in pu. It can be observed that voltage is also quickly regulated at 1pu after the control is started.

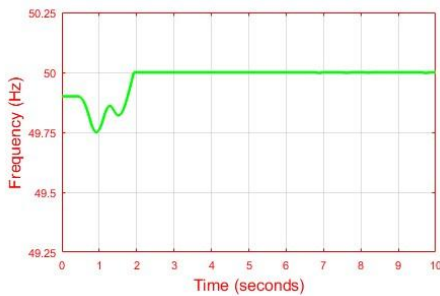
Case-II: PV power is less than load power



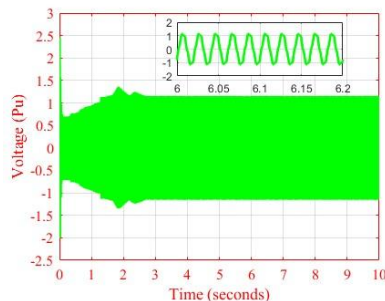
(a)



(b)



(c)

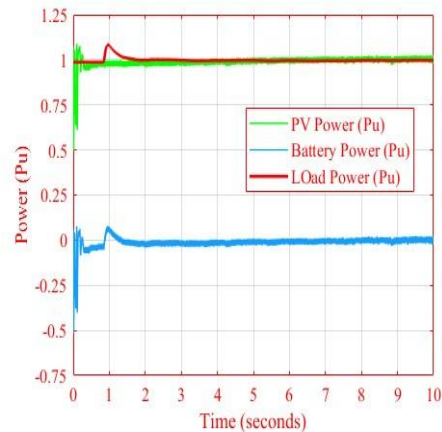


(d)

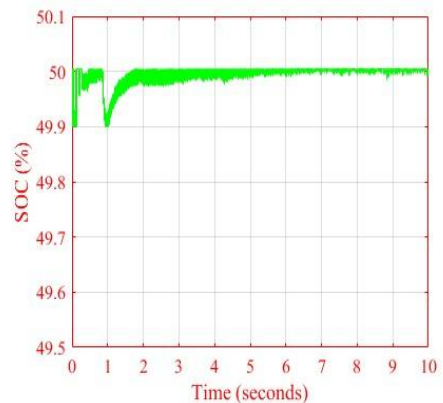
Fig (9). (a)Power (Pu) (b) SOC (%) (c) Frequency (Hz) (d) Positive sequence Voltage (Pu) while PV power is less than load power

When PV power is less than load power the excess power required by load is supplied by battery storage system by discharging the battery. This can be explained by using fig 9(a) and fig 9(b). In fig 9(a) P_u PV power is less than load power. So the excess power is supplied by battery by discharging. The positive power indicates the discharging of battery. In fig 9(b) SOC decreasing with time indicates the discharging of battery. Fig. 9(c) shows the frequency which initially dips to a value of 49.75Hz due to the load-generation imbalance. The frequency control from the PV generator starts within 2sec which quickly regulates the frequency back to 50Hz. Fig 9(d) shows the plot of the positive sequence PCC voltage in pu. It can be observed that voltage is also quickly regulated at 1pu after the control is started.

Case-III: PV power is equal to load power



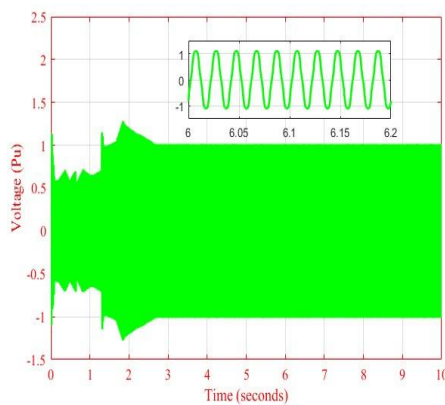
(a)



(b)



(c)



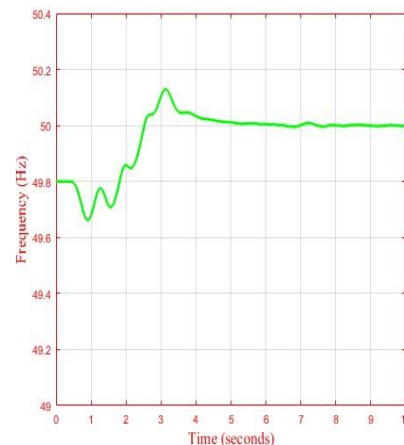
(d)

Fig 10. (a) Power (Pu) (b) SOC (%) (c) Frequency (Hz) (d) Positive sequence Voltage (Pu) while PV power is equal to load power

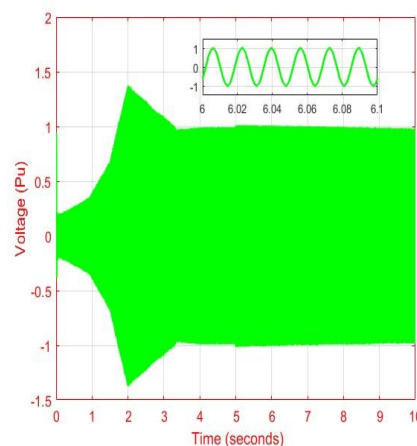
When PV power is equal to load power there is no need of battery storage system. So there is no charging and discharging of the battery. This can be explained by using fig 10(a) and fig 10(b). In fig 10(a) Pu PV power is equal to load power. The zero power indicates the no change of battery. In fig 10(b) constant SOC indicates there is no charging or discharging of battery. Fig 10(c) shows the frequency which initially dips to a value of 49.6Hz due to the load-generation imbalance. The frequency control from the PV generator starts within 2sec which quickly regulates the frequency back to 50Hz. Fig 10(d) shows the plot of the positive sequence PCC voltage in pu. It can be observed that voltage is also quickly regulated at 1pu after the control is started.

V-f control micro source

Fig 11(a) and 11(b) show the results obtained when the micro source like diesel generator is involved in the voltage and frequency regulation of the microgrid and the solar PV is controlled to dispatch constant active and reactive power. Fig. 11(a) shows the frequency of the microgrid which varies in the beginning and then, gradually reached 50Hz and stays at 50 Hz in around 5 sec. It is clear from this figure that the diesel generator takes much longer time to recover the frequency than the PV and battery combination as discussed above. Fig 11(b) shows the voltage plot of the microgrid. It is also clear that it takes around 5sec for the voltage to settle down to 1pu.



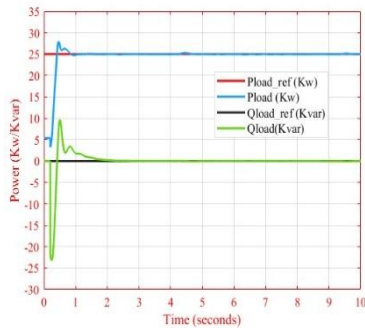
(a)



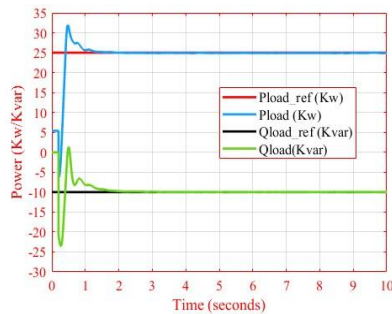
(b)

Fig 11: (a) Frequency (Hz) (b) Positive sequence Voltage (Pu) controlled by Other sources

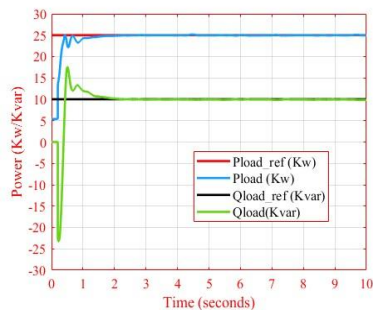
Simulation results of P-Q control



(a)



(b)



(c)

Fig 12. (a) R-load (b) RC-load (C) RL-load P-Q control of inverter

The results of P-Q control with integrated MPPT and battery control is presented in this section. Where P-Q control of R, RL, RC load are three cases respectively.

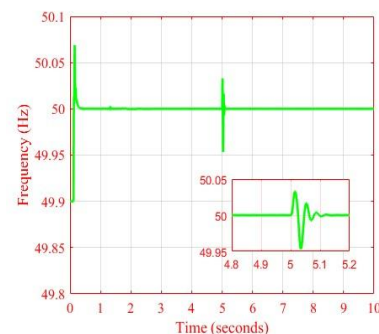
Fig 12(a) illustrates the P-Q control of R load. Here the reference active power and reactive power are 25Kw and is 0Kvar respectively. The power at load terminal was given as shown on fig 12(a). The active and reactive power are followed the reference within a 2sec. It indicates the fast response of P-Q control.

Fig 12(b) illustrates the P-Q control of RC load. Here the reference active power and reactive power are 25Kw and is 10Kvar respectively. The power at load terminal was given as shown on fig 12(b). The active and reactive power are followed the reference within a 2sec. It indicates the fast response of P-Q control.

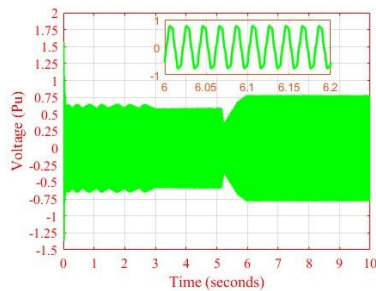
Fig 12(c) illustrates the P-Q control of RL load. Here the reference active power and reactive power are 25Kw and is 10Kvar respectively. The power at load terminal was given as shown on fig 12(c). The active and reactive power are followed the reference within a 2sec. It indicates the fast response of P-Q control.

Transition from P-Q control to V-f control

A separate case study is carried out to show the dynamic characteristics of the proposed V-f and P-Q control algorithms while transitioning from the grid connected (P-Q control) to microgrid (V-f control) structure. The bus is connected to the substation in the grid connected mode and in the islanded case, the tie switch is opened at 5sec. The microgrid is then fed only by the micro source like diesel generator located at the same bus, and the PV generator and battery at another bus. Fig 13(a) shows the frequency of the system and fig 13(b) shows voltage at PCC both in grid connected and islanded cases. It can be observed that the islanded microgrid frequency is quickly revived back to 50 Hz in less than 1sec. A similar response can be observed in the voltage profile at PCC as shown in fig 13(b) This is due to the faster control characteristics of PV and battery integrated system involved in V-f control in islanded case.



(a)



(b)

Fig 13: (a) Frequency (Hz) (b) Positive sequence Voltage (Pu) while transferring from P-Q control to V-f control

VI. CONCLUSION

This work presents strategies of V-f control and P-Q control of for microgrids with PV generator and battery storage. In the control strategies, the PV generator is operated at MPP, and the battery storage acts as a buffer in order to inject and absorb deficit or surplus power by using the charge/discharge cycle of the battery. The paper contributes in demonstrating the control strategies with effective coordination between inverter V-f (or P-Q) control, MPPT control, and battery control. The proposed control strategy also provides a smooth transition of PV side PQ control in grid connected mode to V-f control in islanded mode. The proposed V-f control method shows a very satisfactory performance in reviving highly reduced voltage and frequency back to the nominal values in a matter of only 2 seconds. It is much faster than the micro source like diesel generator control which takes around 5 seconds to settle down.

Hence, PV and battery installations might be applied effectively in restoring the microgrid frequency and the voltage at PCC after disturbances. Similarly, the proposed integrated and coordinated P-Q control algorithm can be effectively used in supplying some critical loads of a microgrid with solar PV and battery.

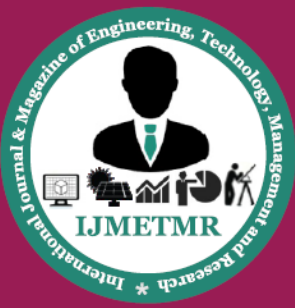
VII. FUTURE SCOPE

In the present methods, the control parameters are dependent upon the PV, battery, and external grid conditions and must be re-tuned with the changing

conditions. This can be overcome by using an adaptive method to obtain these parameters dynamically based on the system conditions. The adaptive control methods could be a very useful and promising future direction of this work.

REFERENCES

- [1] Coordinated V-f and P-Q Control of Solar Photovoltaic Generators with MPPT and Battery Storage in Microgrids by Sarina Adhikari ; Fangxing Li on IEEE Transactions on Smart Grid, 2014, Volume 5.
- [2] Single-phase solar PV system with battery and exchange of power in grid-connected and standalone modes by Nupur Saxena, Bhim Singh, Anoop Lal. Vyas in ietdl.
- [3] J. C. Vasquez, R. A. Mastromauro, J. M. Guerrero, and M. Liserre, "Voltage support provided by a droop-controlled multifunctional inverter," IEEE Trans. Ind. Electron., vol. 56, pp. 4510–4519, 2009.
- [4] H. Li, F. Li, Y. Xu, D. T. Rizy, and J. D. Kueck, "Adaptive voltage control with distributed energy resources: Algorithm, theoretical analysis, simulation and field test verification," IEEE Trans. Power Syst., vol. 25, pp. 1638–1647, Aug. 2010.
- [5] H. Li, F. Li, Y. Xu, D. T. Rizy, and S. Adhikari, "Autonomous and adaptive voltage control using multiple distributed energy resources," IEEE Trans. Power Syst., vol. 28, no. 2, pp. 718–730, May 2013.
- [6] L. D. Watson and J.W. Kimball, "Frequency regulation of a microgrid using solar power," in Proc. 2011 IEEE APEC, pp. 321–326.
- [7] M. G. Molina and P. E. Mercado, "Modeling and control of grid-connected photovoltaic energy conversion system used as a dispersed generator," in Proc. 2008 IEEE/PES Transm. Distrib. Conf. Expo.: Latin America, pp. 1–8.



[8] N. Kakimoto, S. Takayama, H. Satoh, and K. Nakamura, "Power modulation of photovoltaic generator for frequency control of power system," *IEEE Trans. Energy Conv.*, vol. 24, pp. 943–949.

[9] T. Ota, K. Mizuno, K. Yukita, H. Nakano, Y. Goto, and K. Ichiyangi, "Study of load frequency control for a microgrid," in *Proc. 2007AUPEC Power Eng. Conf.*, pp. 1–6.

[10] L. Xu, Z. Miao, and L. Fan, "Coordinated control of a solar battery system in a microgrid," in *Proc. 2012 IEEE/PES Transm. Distrib. Conf. Expo. (T&D)*, pp. 1–7.